P2R2C2

Climate Change Projections for Variables Affecting Road Networks in Europe

Report Nr 6
April 2010

Project Coordinator
University of Nottingham, UK

ZAG, Slovenia

VTT, Finland

SINTEF, Norway

Report Nr 6 – Climate Change Projections for Variables Affecting Road Networks In Europe

End date of project: July 2010

Authors:

Lasse Makkonen - VTT Technical Research Centre of Finland

Jouko Törnqvist - VTT Technical Research Centre of Finland

Jussi Ylhäisi - University of Helsinki

Jouni Räisänen - University of Helsinki

Version: 2

Table of contents

1 Introduction

The global climate change will affect all infrastructure including road networks. The effects will be different in various parts of the world due to differences in climate change and in the structure and properties of the roads. In this report climate change projections are presented for those climate variables that were considered most likely to affect the long-term performance of road networks in Europe. These projections are based on climate simulations by a regional climate model and using two plausible future emission scenarios. The results are presented as maps.

2 The climate simulation method

2.1 Global models

Data from two global climate simulation models, the Hadley Centre HadAM3H (*Had*) and Max-Planck Institute ECHAM4/OPYC3 (*MPI*), were used to drive the numerical regional climate model RCAO. HadAM3H is a high resolution (1.875° longitude x 1.25° latitude) atmosphere model (Gordon et al., 2000) for which the sea surface temperature and sea ice conditions were derived from observations and earlier lower-resolution coupled atmosphere-ocean simulations, as explained by Räisänen et al. (2004). ECHAM4/OPYC3 is a coupled atmosphere-ocean model with a resolution equivalent to a grid spacing of 2.8° longitude x 2.8° latitude (Roeckner et al., 1999).

The global climate models were first run from 1860 to 1990 using observed or estimated changes in the atmospheric composition. From 1990 on, the calculation was continued as two separate simulations using different scenarios of anthropogenic greenhouse gas and sulphur emissions, IPCC SRES A2 and B2 (Nakićenović et al., 2000, Solomon et al., 2007). Both the greenhouse gas and sulphur emissions are larger for A2 than B2, but for long-term changes in the radiation balance, the difference in the cumulative greenhouse gas emissions dominates. Thus, the simulated global warming and the general magnitude of other climate changes in the late 21st century are larger for the A2 than the B2 scenario.

For driving the regional climate model, 30-year periods from both the HadAM3H and *MPI*/ECHAM4/OPYC3 simulations, the "control run" (January 1961 to December 1990) and the "scenario run" (January 2071 to December 2100) were used. The 30-year annual global mean warming predicted by HadAM3H from 1961 - 1990 to 2071 - 2100 is 3.2 °C in scenario A2 and 2.3 °C in scenario B2. The corresponding warming predicted by ECHAM4/OPYC3 is 3.4 °C for A2 and 2.6 °C for B2. These values are in the midrange of the uncertainty interval reported by Meehl et al. (2007). Taking into account a wider range of emission scenarios, model-specific climate sensitivities and uncertainties in the carbon cycle, they projected a global warming of 1.1 to 6.4 °C from 1990 to 2095.

2.2 The Regional Model

The Rossby Centre coupled regional climate model RCAO consists of the atmospheric model RCA2 (Bringfelt et al., 2001) and the Baltic Sea model RCO (Meier et al., 1999, Meier,

2001). The atmospheric model RCA2 originates from version 2.5 of the HIRLAM model (Eerola et al., 1997), but includes many new parameterizations and other changes as explained in Räisänen et al. (2004) and Jones et al. (2004). RCA2 was run in a rotated longitude-latitude grid with a 0.44° (approximately 49 km) resolution in both horizontal directions and with 24 levels in the vertical. The integration domain of RCAO covers an area of $10^6 \times 10^2$ grid squares (see Räisänen et al., 2004). The Baltic Sea model RCO was run with the horizontal resolution of 11 km and with 41 levels in the vertical (see Meier, 2001). The coupling procedure between RCA2 and RCO is described in Döscher et al. (2002).

In the following, the HadAM3H-driven RCAO simulations will be denoted as "*Had*" and the ECHAM4/OPYC3-driven simulations as "*MPI*". The control runs for 1961 - 1990 are denoted by "RCA2" and the scenario runs for 2071 - 2100 with the A2 scenario by "A2", and the scenario runs with the B2 scenario by "B2".

Accordingly, four climate projections were obtained: For two emission scenarios A2 and B2, and both of them as simulated based on boundary conditions from two global climate models *Had* and *MPI*. Results for all these four projections are presented in this report for one variable (freeze-thaw cycles) in order to give some indications of the differences caused by the uncertainty in the future emissions and caused by differences in the climate models. In that connection, the four results are denoted as *Had*-RCA2 A2, *Had*-RCA2 B2, *MPI*-RCA2 A2 and *MPI*-RCA2 B2. Otherwise, the results are given as the mean of the four different simulations. These are denoted as "AB". Since there is no objective way to rate the quality or relevance of the four simulations, we consider that the mean of them, AB, is our "best estimate" of the future regarding the simulated variables.

The variables used in the analysis vary in their temporal resolution. Daily values were used for maximum and minimum temperature, whereas for precipitation and instantaneous temperature the data used had a 6-hour resolution. The analysis was done for both the annual and the seasonal (winter DJF, spring MAM, summer JJA, autumn SON) values. The seasonal values are given as maps in this report for one parameter (freeze-thaw cycles) and discussed for others.

3 Results

The maps of the simulated changes (Figs. 1-6) were produced at the Department of Physics/University of Helsinki. It should be noted that, in some cases (most notably, Fig. 2), spurious features are seen near the map boundaries. These are associated with the relaxation zone used to fit the RCAO simulated fields to the data from the driving global models. Note that all the results are presented as the *change* in the parameter of interest, as computed by a particular model, from its 30-year mean value over the period 1961-1990 to its 30-year mean value over the period 2071-2100. Thus the impact of errors or limitations in the predictive capability of a model at any location are reduced. As such errors are likely to exist both in 2071-2100 and also in 1961-1990, taking the difference in the parameter's value reduces their significance.

Changes in the annual maximum air temperature (Fig. 1) are here defined as the 30-year mean difference (2071-2100 minus 1961-1990) in the highest maximum air temperature of each year, which always occurs during the summer season. In all of the four simulations, the mean of which is shown in Fig. 1, the largest increases are found in Central and Southern Europe with maximum values over France and Germany, whereas air temperature changes in Northern Europe are found to be smaller. The four simulations showed a relatively large effect of the driving global model to regional climate simulations. In the coupled-GCM *MPI*, the increase in sea surface temperatures over the Atlantic Ocean is much larger than in the Hadley models, and this most likely contributes to the larger increase in maximum air

temperatures over western and central Europe in the corresponding RCAO simulations.

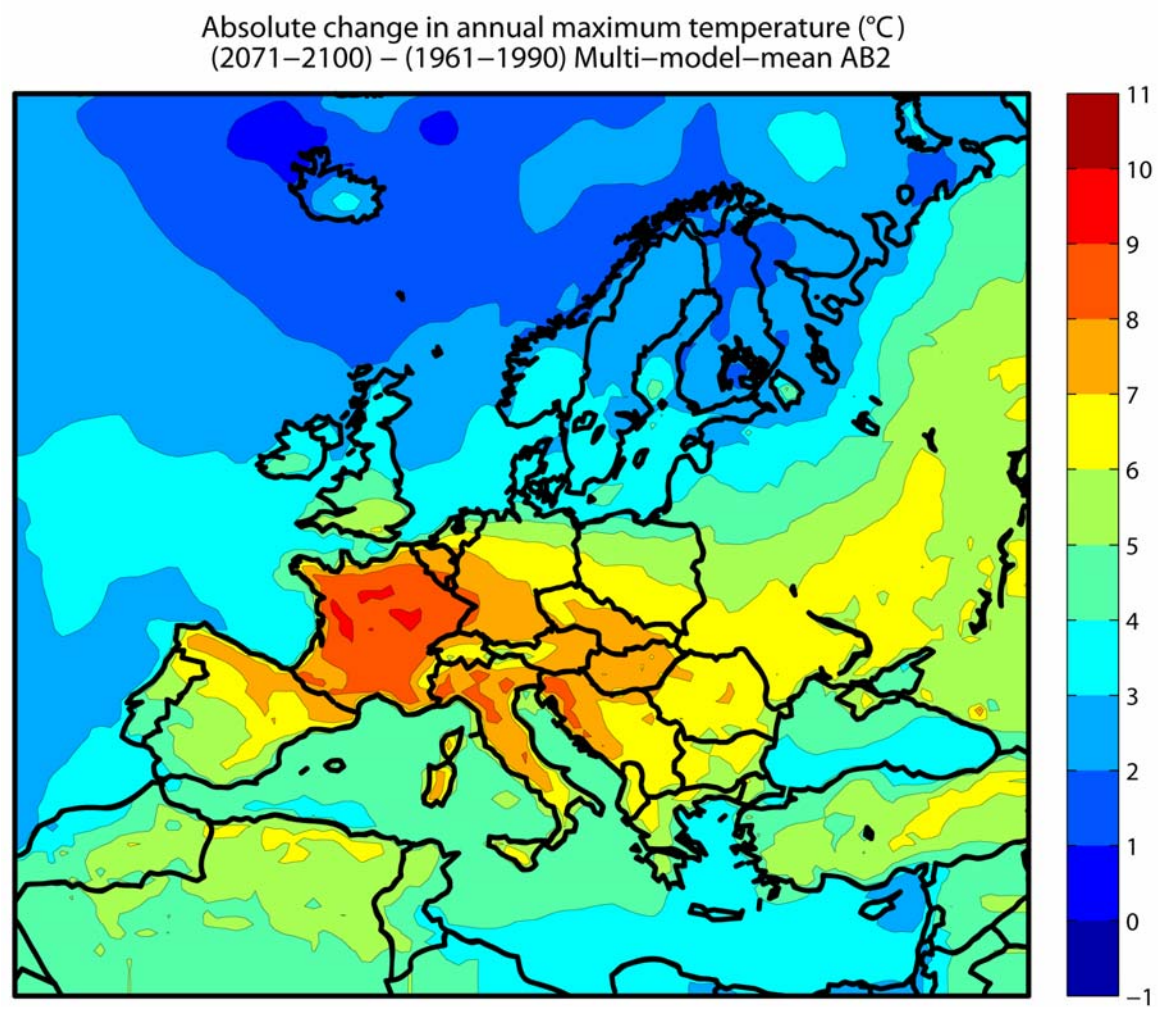

Fig. 1 Change in the annual maximum air temperature (°C)

Figure 2 shows the change in the annual number of events when the average air temperature changes by more than 15 °C in 6 hours. Note that the map does not distinguish between cases of temperature increase and decrease. Most of the rapid, large temperature changes occur in the winter half-year in northern Europe and mountainous area (typically a few cases per year in the present climate) but in summer in the Mediterranean area (typically 20-40 cases). Consequently, the annual changes seen in Fig. 2 are dominated by the changes in these areas and seasons.

In north-eastern Europe and in the Alps, there is a general decrease. This is likely associated with a decrease in snow cover that in the present climate promotes the formation of strong temperature inversions. In southern Europe, the patterns are more mixed. Where an increase is seen, such as that over Italy, this is related to an increase in the average summertime diurnal temperature range. This, in turn, is likely caused by reduced cloudiness and soil moisture, which lead to a more variable radiation climate and less effective evaporative damping of temperature variations.

While qualitatively similar in many respects, the simulations based on the Hadley and *MPI* boundary data exhibit some marked quantitative differences. The large changes near the

southern and eastern boundaries, where the simulated climate is distorted by relaxation effects, are difficult to interpret.

It is important to note, in all these temperature results, that it is air temperature that is being analysed. Absolute pavement temperature is usually higher than the air temperature due to solar gain effects. However, taking the difference in the mean values of the air temperature parameter of interest means that the difference may be closer to the difference that might occur in the pavement.

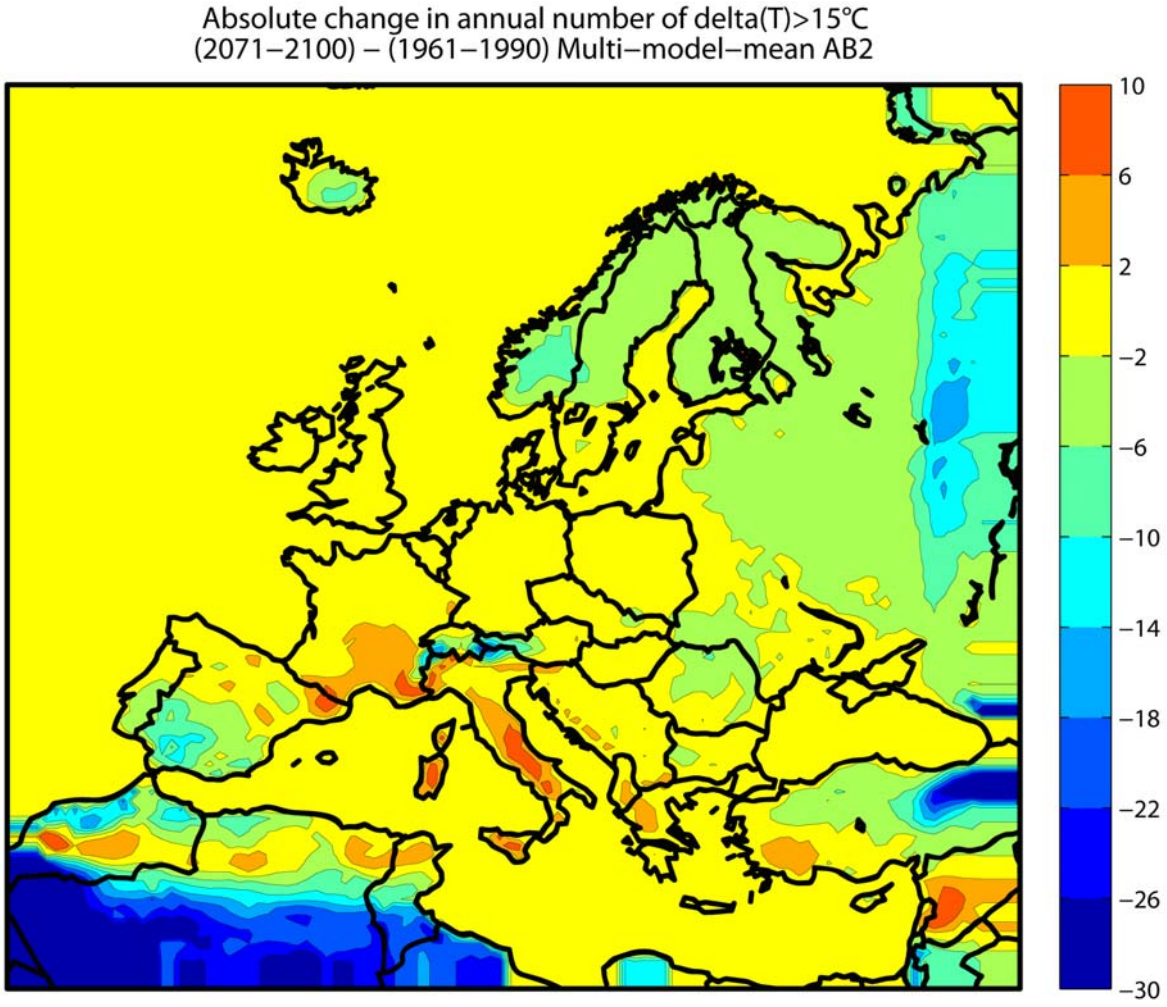

Fig. 2 Change in annual number of cases of temperature change in 6 hours by more than 15 °C

Figure 3 shows the change in the annual integrated cold sum (<0 °C) between the periods 1961-1990 and 2071-2100. This variable is calculated based on daily values of maximum and minimum temperature and the temperature change between these two values was assumed to be linear. The units of the variable are defined as [hour × Kelvin = °C hours] and it is, as expected, dominated by wintertime changes. This index is a nonlinear function of both the length and the severity of the winter, with by far the largest present-day values in the coldest (north-eastern) parts of the area (up to approximately 7×10^4). For this reason, and because the simulated wintertime warming also increases from west to east, the largest decreases are seen in the north-eastern parts of the model domain.

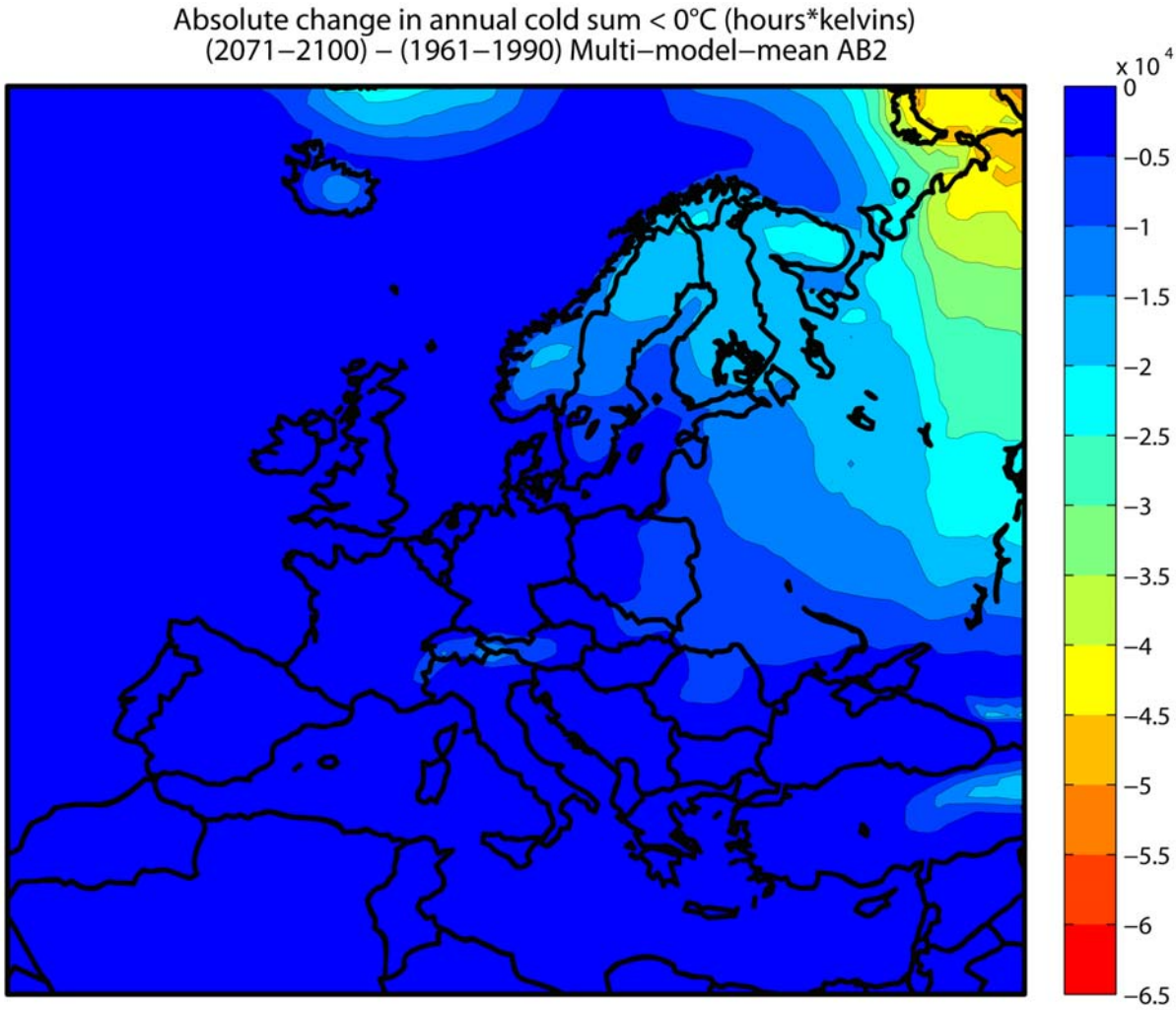

Fig. 3 Change in the annual cold sum (°C hours)

In Figure 4 the annual heat sum is plotted with a threshold temperature of 25 °C. The variable is calculated with same daily data of maximum and minimum temperatures and has the same units [hour × Kelvin = °C hours]. In the present climate this parameter is zero for most of Europe, so that the relative increase is very high in central Europe. Because the sum is unaffected by days with the maximum temperature below 25 °C, and the RCAO model has a slight tendency to underestimate the highest summer temperatures in northern Europe (Räisänen et al. 2003), both the simulated 20th century values and the changes in northern Europe are rather small in absolute terms. Much larger increases occur further south in Europe. This index is also a good example of the dependence of the results on the driving GCM simulation. The larger summer warming in the *MPI* than in the Hadley simulations also leads to a larger increase in the heat sum in southern and central Europe.

As expected, increases in the heat sum mostly occur in the summer season. However, the warming of autumns also seems to contribute substantially to the annual sums in the southern Mediterranean area.

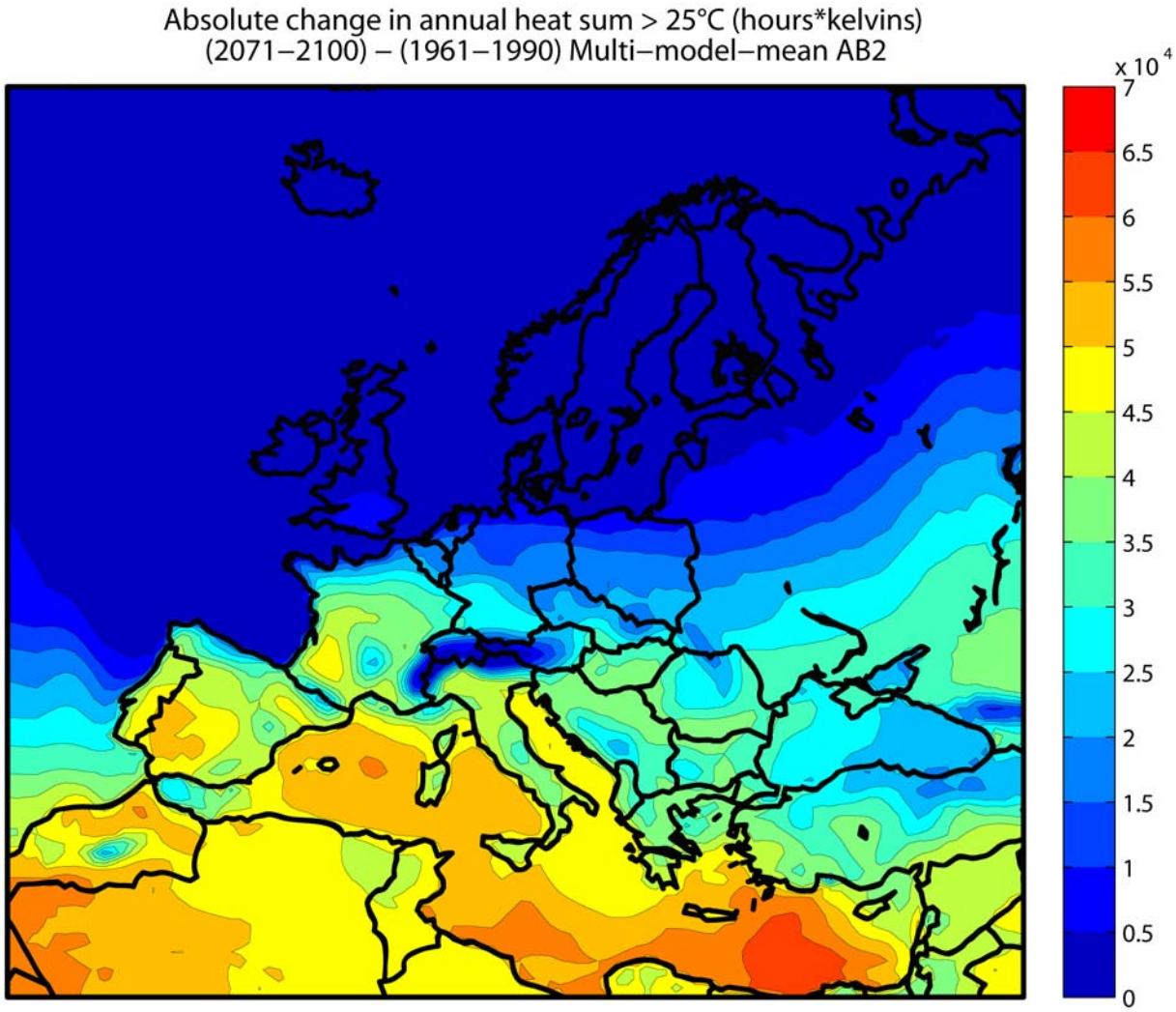

Fig. 4 Change in the annual heat sum (°C hours)

Figure 5 shows the change in the annual number of cases when the temperature crosses the freezing point of zero degrees. This variable is calculated from the 6-hourly temperature data. In the present climate this variable is close to zero in western and southern parts of Europe and up to 130 only in the mountainous regions. The relative change in this variable is therefore, quite significant.

Figure 6 shows the same result in the four simulations. Comparison of figures 5 and 6 gives an impression on how much the simulations based on different emission scenarios and global models differ from each other.

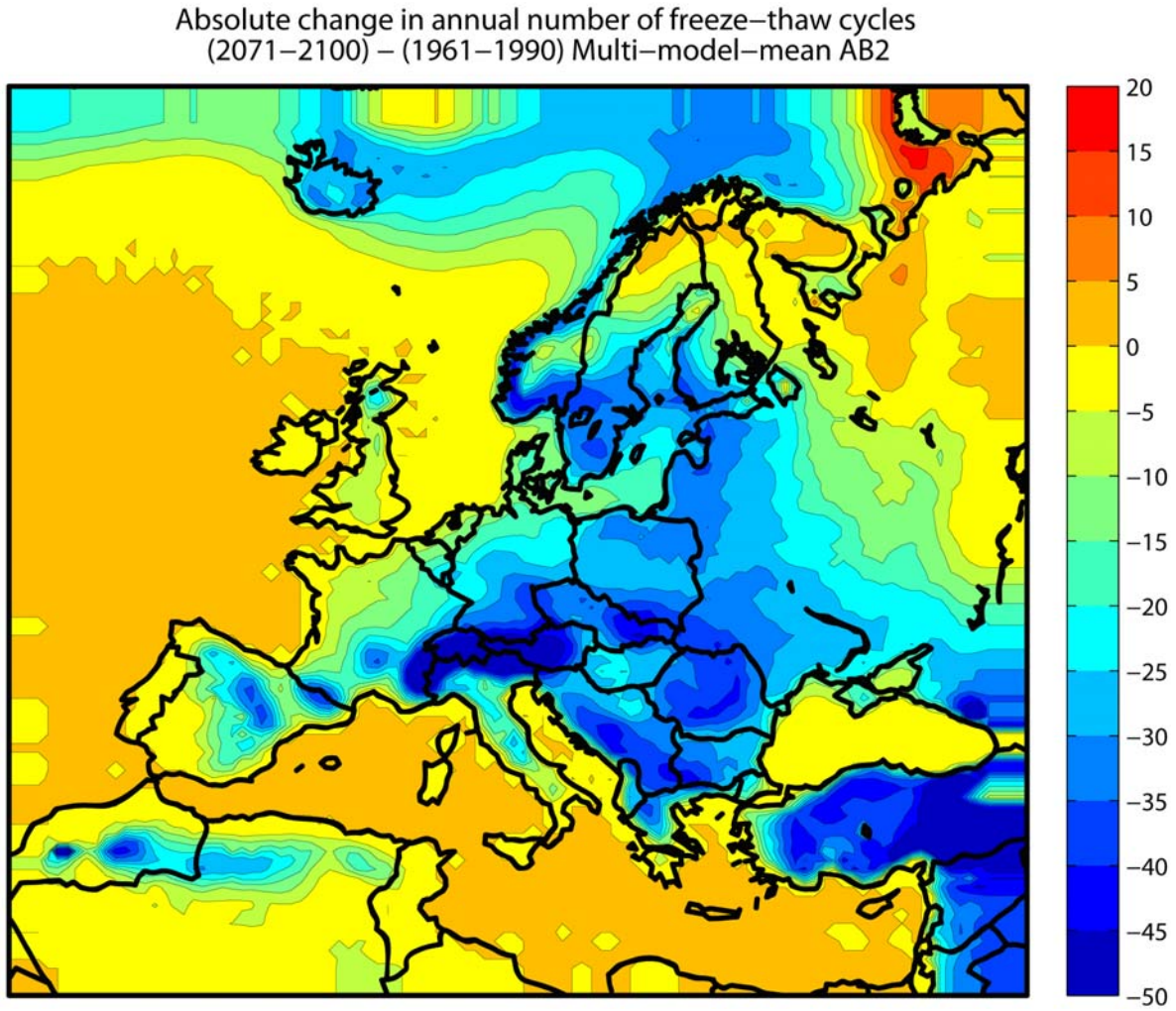

Fig. 5 Change in the number of 0 °C temperature crossings (annual)

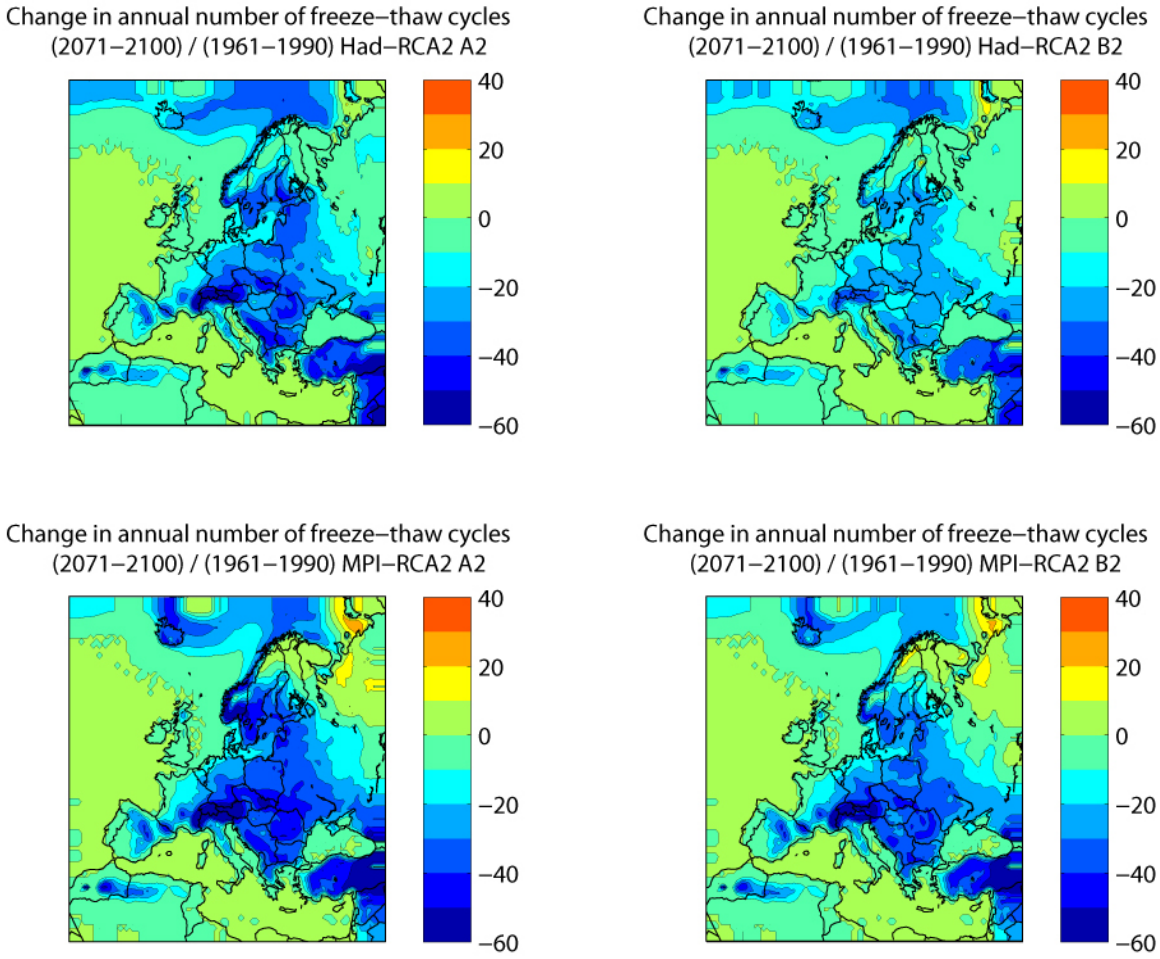

Fig. 6 Change in the number of 0 °C temperature crossings (annual) as simulated by using two different emission scenarios and two different global climate models.

The number of freeze-thaw cycles shows both seasonal and spatial variability, and this is illustrated in figures 7a (winter) and 7b (spring); the contribution of summer and autumn is small for this variable. When looking at the annual maps most areas are bluish in colour, indicating fewer zero-crossings in the future. However, in the coldest, north-eastern parts of the integration area, the situation is not that simple.

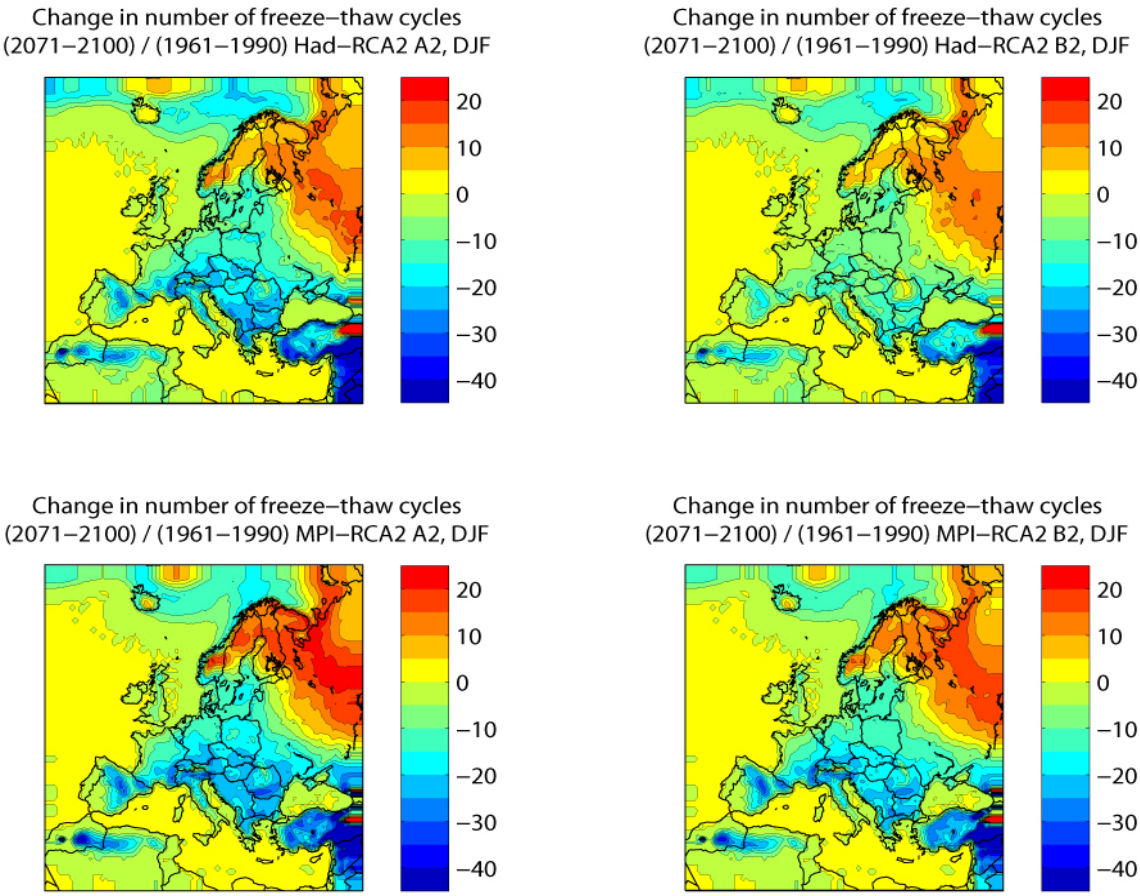

Fig. 7a Change in the number of 0 °C temperature crossings in winter (December, January, February).

In wintertime, the zero-crossings will increase (Fig. 7a), but in springtime they will decrease (Fig. 7b) in the same area. This is because of the climate conditions. In these areas, which are seen as the red belt in the figure 7a, the warming will make the winter temperatures to stay closer to zero in the future. To the northeast of this area, the temperatures will still be cold enough to keep the number of zero-crossing events relatively low, hence a smaller increase is seen there. This finding is quite robust across all of the simulations. In the spring, the belt of increase retards to the extreme northeast of the domain, and is replaced by marked decrease further to the southwest, particularly southern Finland and central Scandinavia, as well as in the Alps. There, the average present-day spring temperatures are already in the present climate close to (or in the end of the spring, well above) zero; consequently a further warming of climate leads to fewer zero-crossings.

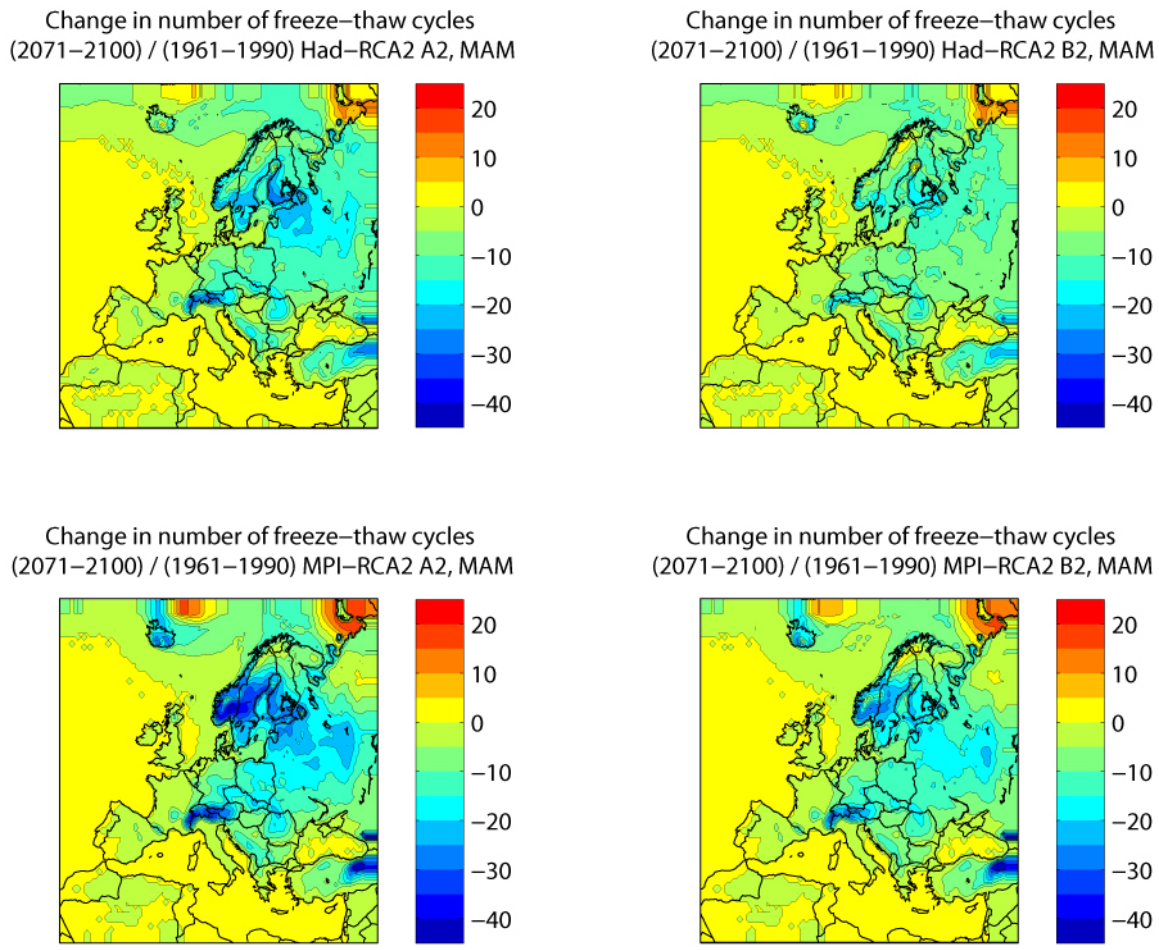

Fig. 7b Change in the number of 0 °C temperature crossings in spring (March, Apri,l May).

Figure 8 shows the projected change in the annual precipitation amount. The present values are in the range of 300 to 2000 mm per year, so that the projected changes represent a very significant relative change, up to 50% in north-eastern Europe and down to -30% in the south.

In annual results the borderline between increasing and decreasing precipitation is not well defined in the *Had*-simulations. In the *MPI*-simulations, the contrast between southern and northern Europe is much sharper. The maps during the wintertime (not shown) look very much the same as those obtained from other simulations within the PRUDENCE (Prediction of Regional Scenarios and Uncertainties for Defining European Climate Change Risks and Effects [Christensen et al., 2007]) project, but the summertime maps seem to show greater declines of precipitation in central Europe. Nevertheless, the general characteristics are all the same. In summer, the precipitation will decrease with the exception of the most northern areas (approximately to the north of 60°N; see Fig. 6 of Räisänen et al. 2004), and in winter precipitation will increase except for the southernmost areas near the Mediterranean. The precipitation change between the two driving models are partly related to different changes in the atmospheric circulation during the winter half-year; in particular, there is a strong increase in time-mean westerly flow in northern Europe in *MPI* that is absent from *Had* (Räisänen et al. 2004). Furthermore, the aforementioned larger increases in Atlantic Ocean surface temperatures in *MPI* than in the Hadley model also most likely contribute to the differences in precipitation change, by providing a larger increase in the moisture content of

air (Kendon et al., 2009).

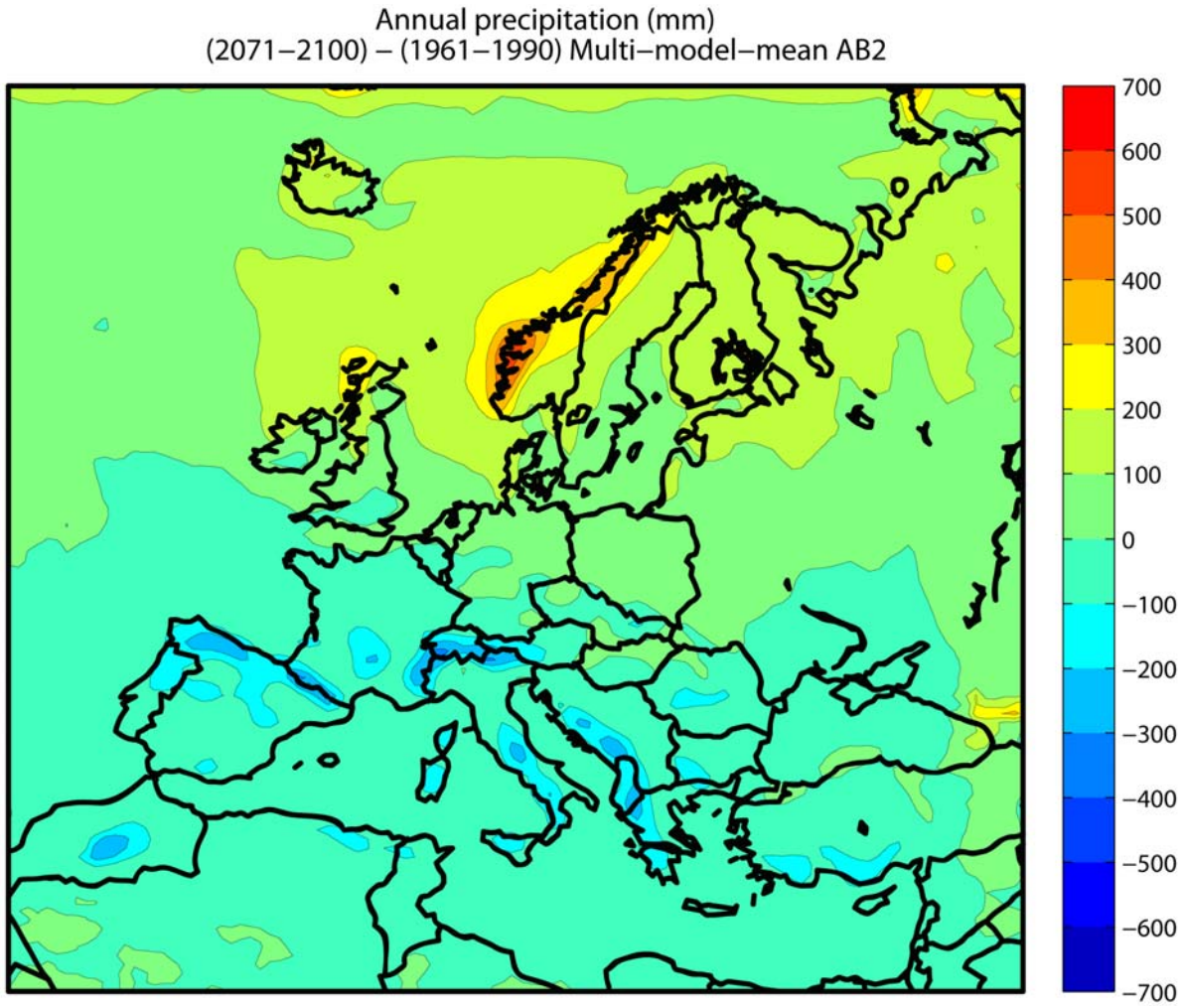

Fig. 8: Change in the annual precipitation.

4 Implications of the results regarding road networks

In this chapter implications from the maps presented in chapter 3 are outlined. Effects on the road network - surface, bridges, drainage and maintenance is considered.

4.1 Change in the annual maximum temperature. (see Figure 1)

4.1.1 Regional patterns of the changes

In all the models and scenarios the greatest change in the annual maximum temperature is observed in Central Europe; In France, in southern parts of Germany, northern Italy and in

the Balkan region: 5 to 12 °C. In Western Europe the change is greater than in the Eastern Europe. In the Mediterranean region and Southern UK the change is not so extreme: 4 to 8 °C. In Northern Europe and Northern UK and Ireland the change is limited to 1 to 6 °C.

4.1.2 Effects

- In the bitumen-coated roads rutting and deformation will significantly increase unless modifications are made to the surface materials in the future. One should most probably be able to adapt to the increase in rutting in roads with a re-paving cycle of less than 20 to 30 years. On thin paved roads the effect also applies to the unbound bearing layers and road base as the softened pavement redistributes the stress caused by traffic loading less effectively than planned. Changing of the pavement material to a more rigid one should be made by the middle of the century on thin paved roads to avoid deformations.
- On concrete paved roads an increase of the seam openings and movements will be observed. Greater movement caused by thermal expansion can be expected and should be compensated by developing construction joint solutions on bridge decking and concrete paved roads. These safety measures should be planned in advance on bridges with a long service life, i.e. one should ensure in advance that temperature difference premises in forced temperature deformations correspond to the future scenarios.

4.1.3 Severity

The graveness of financial and operational consequences as singular phenomena: Western Central Europe 3 and other regions 1 to 2 (scale of 1 to 5).

4.2 The amount of the events per annum in which the change of temperature within six hours is greater than 15 °C. *(see Figure 2)*

4.2.1 Regional patterns of the changes

In Italy, South Western France, possibly in Greece and on islands of the Western Mediterranean the frequency of rapid air temperature changes will increase. In other regions this frequency will remain the same or decrease.

4.2.2 Effects

The phenomenon contributes to forced transformation stress loading, particularly on brittle materials and structural parts with two conjoining different materials (concrete pavement, expansion joint etc.). A rapid change in air temperature which does not directly correspond to a temperature change of surfaces exposed to sun light. However, the observed impact is

similar.

4.2.3 Severity

The graveness of financial and operational consequences as singular phenomena are nearly significant at 2 (on a scale of 1 to 5) in the countries listed above.

4.3 The change of annual cold sum (<0 °C) in h °C. *(see Figure 3)*

4.3.1 Regional patterns of the changes

In Nordic countries and the Baltic countries the annual cold sum will significantly decrease: -15000…20000 h°C. In Southern Sweden and Poland the change is 5000…10000 h°C or less. In other regions the change is insignificant.

4.3.2 Effects

The change presented in the graphs depicts an average change and not an extreme change (e.g. occurring once in 20 or 50 years). However, it is obvious that as the annual cold sum is an accumulated sum, the extreme values will also decrease. A quantification of extreme years cannot be made based on the results depicted here. The change in the annual cold sum has two explicit consequences a) frost penetration depth will change and b) the period of a time while road structure is in frozen state per annum will change. In addition, there is an obvious effect on the existence of winter ice roads.

North of the polar circle the average annual cold sum is less than -40,000 h°C and in the case of the sum occurring in 20 years less than -50,000 h°C. In the average latitude of the Nordic countries the annual cold sums are respectively -20,000 and -35,000 h°C. With a change of +15,000…+20,000 h°C the penetration depth of the frost at the polar circle will decrease by approximately 20% and further to the south by up to 50%. If the change would directly correspond to the annual cold sum of the years with extremely cold conditions, one could, for example, make structures thinner when other prerequisites (load capacity, drainage etc.) are guaranteed.

The change of annual cold sum is mostly due to decrease in the winter length. This means that the decrease of the annual cold sum affects the months during which “rasputitsa”[1] will occur and the decrease of the length of the periods in which extreme heavy load transportation can be executed on low volume roads. A relevant example is that transportation of wood will be possible for shorter periods of time.

The change in a limited area (Lapland) is significant. The affect is mainly beneficent but adverse concerning transportation.

[1] “Rasputitsa” is a word derived from the Russian which literally translates as “Roadlessness”. It indicates the quagmire season when there is a great softening of the road structure caused by a surplus of melted water. It is most marked in the spring.

4.3.3 Severity

The graveness of financial and operational consequences as singular phenomena are significant 2 (scale of 1 to 5) in North Europe. There are both positive and negative influences.

4.4 The change in the annual heat sum in °C hours. *(see Figure 4)*

4.4.1 Regional patterns of the changes

Expect for mountainous areas (the Alps) the h°*C* -hours will increase significantly (3,000-6,000 h°*C*) in the area south of the 50°N latitude. In the 40 °N latitude (Spain, France) the change would be approximately 6,000-7,000 h°*C*.

4.4.2 Effects

The largest consequences will be observed between the 40°N and 50°N latitude, if no adaptations will be made towards the use of deformation resistant surface materials. In such areas – if no adaptations are made and current materials will be used– the deformations will increase significantly. However, the change will occur gradually, with enables to adapt to the change within regular pavement material life cycle. On roads with small traffic load and thin paved roads, the surface material will age more quickly than previously. On bitumen-paved roads the cracking and deformations of the supporting layer will increase.

Evaporation will increase during summer period. The adaptation of roadside vegetation should be commenced in time and maintain the change using observations.

The risk of erosion due to the accumulated effect of dehydrated ground and sudden rain showers will increase. The maintenance work on drainage system and drums will increase.

4.4.3 Severity

The graveness of the financial and operational consequences as a singular phenomenon is significant 3 (1 to 5). Adaptation can be expected.

4.5 Change in number of freeze-thaw cycles. *(see Figures 5-7)*

4.5.1 Regional patterns of the changes

The amount of freeze-thaw cycles will decrease in both global model projections and scenarios except for the northernmost Europe, in particular Lapland.

4.5.2 Effects

The amount of freeze-thaw cycles will incur due to thermal expansion of water upon freezing initiating cracking and cumulative damage of pavements and other porous materials.

In most regions of Europe the change is beneficent and will decrease the pace of surface material degradation. A change in the air temperature does not directly correspond to a change in the surface material temperature, but the change is similar.

The combined effect of changes in this phenomenon and precipitation must be taken into consideration.

The need to counteract slipperiness will decrease in most regions. In Nordic countries one must take into consideration different changes within the countries. There is no need for advance measures.

4.5.3 Severity

The graveness of financial and operational consequences as a singular phenomenon are insignificant or beneficent 1 (1 to 5). Adaptation will be possible by normal follow up procedures.

4.6 Change in annual precipitation. *(see Figure 8)*

4.6.1 Regional patterns of the changes

Annual precipitation will increase in the regions north of the 55th latitude, but it will decrease further to the south. In particular, the decrease will occur in mountainous areas. The absolute increase shown by Fig, 8 in the coastal areas of Norway is great, but when one takes into consideration the current, relatively large annual precipitation, the change is not so significant. However, the relative change is in the order of magnitude of 30% to 40% in many areas. A more significant effect is an increase of precipitation in a region stretching from Central Europe to Northern Europe and especially in regions bordered with the Atlantic Ocean, mountainous and elevated areas (only the model *MPI*). The increase of the annual precipitation is, based on the model results, mainly due to an increase of heavy rain spells.

4.6.2 Effects

A decrease in the annual precipitation, increase of heat periods and increase of temperate days will accumulatively affect especially the drainage on structures and surface layers. The effect is not only positive; the erosion susceptibility due to heavy rain spells will increase and the internal cohesion of unbind material will decrease. The most significant changes will occur on the road slopes and the surface areas of roads.

The increase in precipitation together with increase in heavy rain spells will lead to road base water saturation, overloading of the drainage system, drifting of the ground material and local cave-ins on extreme cases due to erosion initially caused by flooding and affected by water saturation of structures. The water saturation of natural slopes will also increase the risk of a

stability loss on roads located in sloping terrain.

Correspondingly, water loads on bridges and drums and flowing water will increase degradation of circumferential fill in ground and middle support material. This can in extreme cases lead to safety hazard to bridges.

4.6.3 Severity

In Northern Europe (with increasing heavy rain spells) the effect is significant, 3 to 4 even extreme 5 (scale 1…5). The increase in precipitation must be taken into consideration in advance planning, especially concerning structures that are difficult to replace, i.e. having long design life. The required level of advance measures and optimal timing will be hard to predict unless systematic bridge- and route-specific risk assessments are made.

5 Conclusions

Conclusions of the climate model results and their analysis are summarized in Table 1.

Table 1. Conclusions of the effects in a changing climate

Implication	Where significant	Effects & Severity	Adaptation needs
Change in the annual maximum temperature	Western Central Europe, Italy, Balkan	Rutting deformations expansion of joints Severity: 3	For roads adaptation with time Bridges: early adaptation
Change in the number of events per annum in which the change of temperature within six hours is greater than 15 °C	Mediterranean area from Greece to France	Forced deformation, service life of brittle materials, expansion joints Severity: 2	Bridges: early adaptation
Change in the annual cold sum	Nordic Countries, Baltic states	Frost penetration: positive effect Bearing capacity in wintertime (heavy transport) Severity: 2	Adaptation with time
Change in the annual heat sum	Mountainous areas, Spain, France	Deformations on bitumen-paved roads, vegetations and indirect erosion risk Severity: 3	Adaptation with time
Change in number of freeze-thaw cycles	Northernmost Europe	Lapland: negative, other regions beneficent Severity: 1	Adaptation with time
Change in the annual precipitation	North, Northwestern Atlantic coastal areas	Severity: 3…5	Timing of adaptation based on risk analysis

Further studies should be made using the climate models, for example corresponding analysis can be made for extreme events (Makkonen et al., 2007).

In this study, only variables that are directly obtained from the climate model simulation data were used. The selected variables undoubtedly correlate with real problems on roads and, therefore, indicate the consequences of the global climate change on road networks. They are, however, only overall indicators of the factors that are important.

A more specific approach would be possible and should be considered in the future. It is quite feasible to combine a physical or a statistical model of a certain road infrastructure degeneration process with climate model data analysis. The simulation of that process would then proceed on six our basis over many decades. Such a technique would make it possible to simulate locally and in a process specific way the degeneration with time and investigate in detail how different processes respond to the projected climate change.

6 References

Bringfelt, B., Räisänen, J., Gollvik, S., Graham, L.P., Ullerstig, A., 2001. The land surface treatment for the Rossby Centre regional atmospheric climate model - version 2 (RCA2), SMHI Reports Meteorology and Climatology, **98**, Swedish Meteorological and Hydrological Institute, 40 pp.

Christensen, J.H., Christensen, O.B., 2007: A summary of the PRUDENCE model projections of changes in European climate by the end of this century. Clim. Change 81: 7-30.

Döscher, R., Willén, U., Jones, C., Rutgersson, A., Meier, H.E.M., Hansson, U., 2002. The development of the coupled ocean-atmosphere model RCAO. *Boreal Env. Res*., **7**, 183-192.

Eerola, K., Salmond, D., Gustafsson, N., Garcia-Moya, J-A., Lönnberg, P., Järvenoja, S., 1997. A parallel version of the HIRLAM forecast model: strategy and results. Proc. 7th ECMWF Workshop on the use of parallel processors in meteorology. World Sci. Publ., p. 134-143

Gordon, C., Cooper, C., Senior, C.A., Banks, H., Gregory, J.M.,, Johns, T.C., Mitchell, J.F.B., Wood, R.A., 2000. The simulation of SST, sea ice extent and ocean heat transport in a version of the Hadley Centre coupled model without flux adjustments, *Clim. Dyn*., **16**, 147-166.

Jones, C.G., Willén, U., Ullerstig, A., Hansson, U., 2004. The Rossby Centre Regional Atmospheric Climate Model, Part I: Model climatology and performance for the present climate over Europe, *Ambio*, **33**, 199-210.

Kendon, E.J., Rowell, D.P., Jones, R.G., 2009. Mechanisms and reliability of future projected changes in daily precipitation. *Clim. Dyn., published online.*

Makkonen, L., Ruokolainen, L., Räisänen, J. Tikanmäki, M., 2007. Regional climate model estimates for changes in Nordic Extreme events*. Geophysica*, **43**, 19-42.

Meehl, G.A., T.F. Stocker, W.D. Collins, P. Friedlingstein, A.T. Gaye, J.M. Gregory, A. Kitoh, R. Knutti, J.M. Murphy, A. Noda, S.C.B. Raper, I.G. Watterson, A.J. Weaver and Z.-C. Zhao, 2007: Global Climate Projections. In: Climate Change 2007: The Physical Science Basis.Contribution of Working Group I to the Fourth Assessment Report of the Intergovernmental Panel on Climate Change [Solomon, S., D. Qin, M. Manning, Z. Chen, M. Marquis, K.B. Averyt, M. Tignor and H.L. Miller (eds.)]. Cambridge University Press,

Cambridge, United Kingdom and New York, NY, USA, p. 747-845.

Meier, H.E.M., 2001. On the parameterization of mixing in 3D Baltic Sea models, *J. Geophys. Res*., **106**, 30997-31016.

Meier, H.E.M., Döscher, R., Coward, A.C., Nycander, J., Döös, K., 1999. Rossby Centre regional ocean climate model: model description (version 1.0) and first results from the hindcast period 1992/1993, SMHI Reports Oceanography 26, Swedish Meteorological and Hydrological Institute, Norrköping, Sweden, 102 pp.

Nakićenović, N., Alcamo, J., Davis, G., de Vries, B., Fenhann, J., Gaffin, S., Gregory, K., Grubler, A., Jung, T.Y., Kram, T., La Rovere, E.L., Michaelis, L., Mori, S., Morita, T., Pepper, W., Pitcher, H., Price, L., Raihi, K., Roehrl, A., Rogner, H-H., Sankovski, A., Schlesinger, M., Shukla, P., Smith, S., Swart, R., van Rooijen, S., Victor, N., Dadi, Z., 2000. Emission Scenarios. A Special Report of Working Group III of the Intergovernmental Panel on Climate Change, IPCC, Cambridge University Press, 599 pp.

Räisänen, J., 2001. The impact of increasing carbon dioxide on the climate of northern Europe in global climate models (in Finnish with English abstract and figure and table captions), *Terra*, **113**, 139-151.

Räisänen, J., Hansson, U., Ullerstig, A., Döscher, R., Graham, L.P., Jones, C., Meier, M., Samuelsson, P., Willén, U., 2003. GCM driven simulations of recent and future climate with the Rossby Centre coupled atmosphere - Baltic Sea regional climate model RCAO. SMHI Reports Meteorology and Climatology, No. **101**, Swedish Meteorological and Hydrological Institute, 61 pp.

Räisänen, J., Hansson, U., Ullerstig, A., Döscher, R., Graham, L.P., Jones, C., Meier, M., Samuelsson, P., Willén, U., 2004. European climate in the late 21st century: regional simulations with two driving global models and two forcing scenarios, *Clim. Dyn*., **22**, 13-31.

Rockner, E., Bengtsson, L., Feichter, J., Lelieved, J., Rodhe, H., 1999. Transient climate change simulations with a coupled atmosphere-ocean GCM including the tropospheric sulfur cycle, *J. Clim*., **12**, 3004-3032.

Semenov, V.A., Bengtsson, L., 2002. Secular trends in daily precipitation characteristics: greenhouse gas simulation with a coupled AOGCM, *Clim. Dyn*., **19**, 123-140.

Solomon, S., Qin, D., Manning, M., Chen, Z., Marquis, M., Averyt, K.B., Tignor, M., Miller, H.L. (eds.), 2007. Climate Change 2007: The Physical Science Basis. Contribution of Working Group I to the Fourth Assessment Report of the Intergovernmental Panel of Climate Change, IPCC, Cambridge Univ. Press, 996 pp.